Nanoscale Res Lett (2007) 2:373–384
DOI 10.1007/s11671-007-9083-3

NANO REVIEW

Bio-nanopatterning of Surfaces

Paula M. Mendes · Chun L. Yeung · Jon A. Preece

Received: 1 June 2007 / Accepted: 19 July 2007 / Published online: 4 August 2007

Abstract Bio-nanopatterning of surfaces is a very active interdisciplinary field of research at the interface between biotechnology and nanotechnology. Precise patterning of biomolecules on surfaces with nanometre resolution has great potential in many medical and biological applications ranging from molecular diagnostics to advanced platforms for fundamental studies of molecular and cell biology. Bio-nanopatterning technology has advanced at a rapid pace in the last few years with a variety of patterning methodologies being developed for immobilising biomolecules such as DNA, peptides, proteins and viruses at the nanoscale on a broad range of substrates. In this review, the status of research and development are described, with particular focus on the recent advances on the use of nanolithographic techniques as tools for biomolecule immobilisation at the nanoscale. Present strengths and weaknesses, as well future challenges on the different nanolithographic bio-nanopatterning approaches are discussed.

Keywords Lithography · Bio-nanopatterning · Bionanotechnology · Self-assembled monolayers · Biomolecules

P. M. Mendes (✉)
Department of Chemical Engineering, University of Birmingham, Edgbaston, Birmingham B15 2TT, UK
e-mail: p.m.mendes@bham.ac.uk

C. L. Yeung · J. A. Preece
School of Chemistry, University of Birmingham, Edgbaston, Birmingham B15 2TT, UK

Introduction

Bio-nanopatterning of surfaces have been [1–4] of growing interest in recent years, from both scientific and technological points of view. Such artificial biological surfaces can be tremendously useful in diverse biological and medical applications, including nanobiochips, nanobiosensors, tissue engineering, drug screening, and fundamental studies of molecular and cell biology [1–7]. Biomolecule nanoarray technology not only offers the reward of smaller biochips with more reaction sites, but also smaller test sample volumes and potentially higher sensitivity and throughput screening for molecular diagnostics [8–11]. With the advent of DNA hybridisation nanoarrays comes the remarkable ability to rapidly and effectively monitor the expression levels of thousands of genes to diagnose and treat illness [1]. In comparison with DNA nanoarrays, protein nanoarrays offer the possibility of developing a rapid global analysis of an entire proteome, leading to protein-based diagnostics and therapeutics [1, 2]. Another area that will profit from this novel platform technology, thanks to its flexibility in terms of pattern shape/geometry, is the study of cell adhesion and motility [12].

These broad range of biological and medical applications present many challenging materials-design concepts [1, 2, 4–7]. Prominent among these concepts is the need for (1) positioning distinct biomolecules within designated nanoregions in a substrate with well-defined feature size, shape, and spacing, while retaining their native biological features and properties and (2) high biomolecule resistively by the other regions of the substrate. The past few years has witnessed the advent of several promising strategic methodologies for the aforementioned needs, which are due primarily to the important advances in nanofabrication technology.

Molecular surface science has greatly contributed to the advancement of nanofabrication technology by providing ideal platforms for engineering surfaces on a molecular level [13–18]. For instance, self-assembled monolayers (SAMs), which form spontaneously by the adsorption of an active surfactant onto a solid surface, possess important properties of self-organisation and adaptability to a number of technologically relevant surface substrates. The properties of a SAM (thickness, structure, surface energy, stability) can be easily controlled and specific functionalities can also be introduced into the building blocks. SAMs of thiols on gold [19] and triethoxysilanes on silicon dioxide (SiO_2) [20] are examples of two widely used systems to modify the surface properties of metallic and inorganic substrates.

The variety of methods [21–25] available to characterise SAMs and other functionalised surfaces with nanoscale precision has grown in step with the ability to create sophisticated, nanopatterned surfaces. Scanning probe techniques, such as scanning–tunnelling microscopy [26] and atomic force microscopy (AFM) [27] are very important analytical tools that are capable of imaging surfaces down to the nanometre scale. Aside from their use of nanoscale topographical imaging [28], scanning probe microscopes have been widely employed in nanolithography. Furthermore, lithographic techniques developed for the semiconductor industry, such as electron-beam lithography (EBL), have been combined with advanced surface chemistry techniques to develop new nanofabrication protocols [29–31].

Currently a number of methodologies exist for generating nanoscale features of biomolecules that rely primarily on the aforementioned nanolithographic techniques. Other methodologies have also been reported that relate with bottom–up self-assembly approaches [32–38], redox control [39], conductive AFM [40], scanning-near field photolithography [41] and stamping techniques, such as imprinting lithography [42–44]. A comprehensive review of recent efforts in all these directions is beyond the scope of this review. We instead narrow our focus to five promising nanolithographic approaches, which include dip-pen nanolithography (DPN), nanoshaving, nanografting, EBL and nanocontact printing (nCP) (Fig. 1). These patterning techniques have been employed to either indirectly (processes A, C, D, F and G—Fig. 1) or directly (processes B, E and H—Fig. 1) immobilise biomolecules on surfaces. In the indirect approach, the patterned surfaces are used in a second stage, i.e. post-patterning process (processes I, J, L and M—Fig. 1), as templates to immobilise the biomolecules. The current state-of-the-art as well as the potential and the limitations of these different nanolithographic approaches are discussed.

Dip-pen Nanolithography

Dip-pen nanolithography [45] is a scanning probe nanopatterning technique in which an AFM tip is used to deliver nanoscale materials directly to nanoscopic regions of a target substrate. The deposition process involves the inking of an AFM tip with the nanoscale material, which is then transferred to the substrate by bringing the AFM tip in contact with the substrate surface. Once in contact with the surface, the AFM tip can be either removed from the surface to form dots of the nanomaterial, or scanned across the surface before being removed, resulting in line patterns. The inked AFM tip is most commonly scanned across the substrate in contact mode, however, there have been reports of the AFM tip being scanned in tapping mode [46, 47] to form nanopatterns. Although the exact tip-substrate transport mechanism remains unclear, there is some evidences that the ink transport from the tip is mediated by a water meniscus that forms between the tip and the surface under atmospheric conditions [45, 48–50]. Among other factors, water meniscus properties, the tip geometry, the chemical nature of the ink and substrate, substrate morphology, tip-substrate contact time and writing rate have been demonstrated [45, 50–57] to have a great effect on the resolution and contrast of the patterns formed. Early results showed that DPN could be used to pattern alkanethiol SAMs onto gold surfaces with dot features as small as 15 nm [51]. Each dot was formed by holding a 16-mercaptohexadecanoic acid (MHA)-coated tip in contact (relative humidity 23%) with the gold surface for 10 s.

Parallel probe arrays, which have previously been investigated for use in data storage [58], have allowed DPN to develop into a parallel process [51, 59–66]. The use of tip arrays has been shown to be a technique that can pattern over square centimetres [59, 67], while still retaining nanoscale control of the features. For instance, a 55,000-pen, two-dimensional array has been fabricated [67] that allowed to reproduce the face of Thomas Jefferson, from a 2005 US five-cent coin, 55,000 times with nanoscale resolution. Perhaps more significantly, approximately 4.7×10^8 nanofeatures were used to generate the replicas, and the total time required to perform this fabrication was less than 30 min. This example of nanostructures formed by DPN using parallel probes highlights the potential of DPN as a high-throughput, commercial technique for applications in the fabrication of bioarrays, for example.

Since DPN offers the ability of routinely working in the sub-100 nm regime under ambient conditions, which are critical for patterning biologically active molecules, several different approaches have been investigated for bio-nanopatterning of surfaces using this technique. DPN has been exploited as a tool for indirect immobilisation or direct write of biomolecules on surfaces.

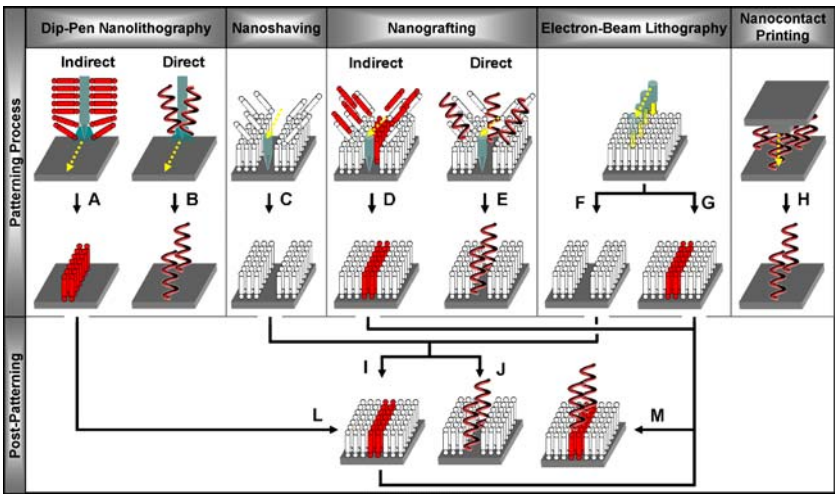

Fig. 1 Schematic representation of the different lithographic techniques employed to indirectly or directly immobilise biomolecules on surfaces at nanometre scale resolution. In the indirect approach, the nanopatterns created by the different lithographic techniques are used in a second stage (i.e. post-patterning process) as templates to immobilise the biomolecules on surfaces

Indirect DPN

In the indirect approach (process A—Fig. 1), the DPN is used as a tool for preparing affinity arrays out of small organic molecules that can subsequently direct the immobilisation of biomolecules from solution onto the patterned surface. Indirect patterning of biomolecules without loss of activity requires the ability to immobilise these biomolecules through specific interactions that minimise non-specific binding. Electrostatic interactions have been successfully exploited to immobilise the negatively charged DNA [68, 69] and negatively charged membrane protein complexes [70] onto protonated amino-terminated nanotemplates generated by DPN. Carboxylic acid-terminated monolayers, which exhibit a high affinity for proteins such as immunoglobulin G (IgG), lysozyme and retronectin, have also been combined with DPN to create protein nanostructures (85–350 nm resolution) on gold surfaces [71–73]. First, gold surfaces were patterned with MHA SAMs, and the unpatterned regions were passivated with a protein-resistant oligoethylene glycol (OEG)-terminated alkanethiol SAM [71]. The proteins were then adsorbed on the preformed MHA arrays while retaining their specificity and biological activity. Nanoarrays of retronectin, a cellular adhesion protein, with dots of 200 nm in diameter and separated by 700 nm were further exploited to study cellular adhesion at the nanometre scale.

In addition to proteins, patterned acid-terminated monolayers have also been used as affinity templates for immobilising mutant cowpea mosaic virus (CPMV) [74] and tobacco mosaic virus (TMV) on gold surfaces [75]. The latter being immobilised at single-level on the surface with the presence of only one TMV particle on each MHA patterned feature (Fig. 2) [75]. The immobilisation approach relied on the coordination of Zn^{2+} metal ions first with the acid groups on the DPN patterned surface and subsequently with the carboxylate-rich TMV surface.

Coupling reactions have also been investigated to immobilise biomolecules on patterned surfaces. DNA [76] and peptide [77] nanoarrays have been fabricated by conjugating, through amide bond formation, amine-containing peptides and DNA to acid-terminated surfaces nanopatterned by DPN. Parallel DPN patterning has also been combined with amine-reactive thiol monolayers to generate arrays of biologically active proteins over a distance of one centimetre [78]. First, a SAM of 11-mercaptoundecanoyl-*N*-hydroxysuccinimide was patterned onto gold using multiple-pen cantilever arrays, and the unpatterned regions

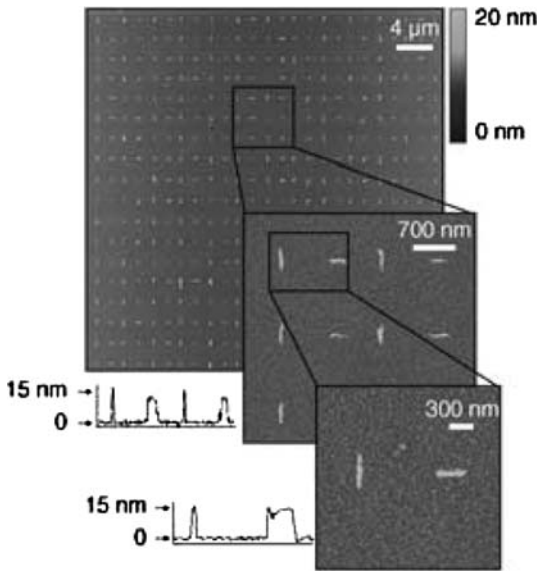

Fig. 2 Atomic force microscopy tapping mode images of site-isolated single TMV virus particles perpendicular to each other [75]

were passivated with the protein-resistant OEG-terminated alkanethiol SAM. The *N*-hydroxysuccinimidyl ester patterned surfaces were then reacted with primary amine groups in the protein A/G to generate nanoscale arrays of protein structures. Antibodies were subsequently adsorbed on the protein A/G nanopatterns and their biological activity demonstrated by using complementary fluorescently labeled antibodies. Although this approach was limited to the immobilisation of one type of protein, it demonstrated the capability of DPN to produce protein-array templates in a relatively high-throughput manner.

Conjugation through amide bond formation was also combined with DPN to covalently bind amino-terminated biotin derivates to chemically activated MHA SAM nanopatterns [79]. The protein streptavidin was subsequently linked to the biotin-terminated patterns, providing a platform for molecular recognition-mediated immobilisation of biotinylated proteins from solution. The widespread availability of biotinylated biomolecules makes this platform particularly attractive. Streptavidin is a tetrameric protein which binds four molecules of biotin with extremely high affinity ($K_a \sim 10^{13}\ M^{-1}$) [80]. Thus, the attachment of streptavidin to the biotin-terminated patterns leaves some biotin unoccupied binding sites, which can be used subsequently to pattern other biomolecules that are conjugated with biotin. In order to demonstrate the potential of this bioconjugation strategy, a streptavidin nanopatterned surface was incubated with a biotinylated bovine serum albumin (BSA) protein. This study confirmed the highly specific molecular recognition interaction between the streptavidin on the surface and the biotin-conjugated BSA [79]. The interaction between biotin nanopatterned surfaces and a related protein, neutravidin, has also been exploited by first covalently immobilising amine-reactive *N*-hydroxysuccinimide functionalised biotin onto amino-terminated monolayers [81].

Another important coupling reaction that has been employed in conjunction with DPN is based on the covalent linkage between thiol and maleimide groups to afford a stable thioether bond [74, 82, 83]. For instance, DPN was used to generate a pattern of circular features (150 nm in diameter) that presented thiol-reactive maleimide groups at low density among penta-(ethylene glycol) groups [74]. CPMV particles that were first engineered to express cysteine thiol groups at the vertices of the icosahedral virus capsid were then chemospecifically immobilised on the preformed patterned circular features.

Direct DPN

Although direct DPN patterning of biomolecules (process B—Fig. 1) offer many potential advantages over indirect immobilisation (e.g. complete absence of non-specific binding and generation of multicomponent arrays with increased complexity), it also poses several challenges. Prominent among these challenges is the need for methodologies that facilitate the transport of the high molecular weight biomolecules from a coated tip to a substrate without sacrificing the sub-100 nm resolution and patterning speed. Furthermore, DPN methodologies are required that preserve the biological activity of the biomolecules during the direct biomolecular patterning. Different strategies have been investigated and it has been found that humidity [52, 84–86], modified AFM tips [52, 84–87] and affinity template surfaces [46, 47, 52, 84–91] are important parameters for controlling the biomolecule nanopatterning process. For example, relative humidity values as higher as 80–90% have been reported to be necessary for a consistent tip-substrate transport of proteins and subsequent optimum patterning results [52, 84].

AFM cantilevers have been chemically modified and employed to immobilise DNA [86] and proteins [52, 84, 85, 87] on surfaces in a direct-write fashion. Improved control over DNA patterning was achieved through surface modification of a silicon nitride AFM cantilever with 3-aminopropyltrimethoxysilane, which promotes reliable adhesion of the DNA ink to the tip surface [86]. Using these modified AFM tips, patterns of DNA on both gold (Fig. 3a) and oxidised silicon substrates (Fig. 3b) were fabricated at sub-100 nm length scale. Thiol-modified DNA molecules were patterned on gold and oligonucleotides bearing 5′-terminal acrylamide groups were patterned on 3-mercaptopropyltrimethoxysilane-modified SiO_2 substrates. Using direct DPN, it was possible to pattern a two-component DNA array on the oxidised silicon substrate and demonstrate its sequence-specific activity by hybridisation with complementary fluorophore-labeled probes (Fig. 3c).

Chemically modified AFM tips have also been successfully exploited to pattern proteins directly on bare gold surfaces with features of 45 nm [52]. The modification procedure involved first the functionalisation of the backside of a gold-coated cantilever with a protein-resistant OEG-terminated alkanethiol SAM. Then, the silicon nitride tip was selectively coated with gold and rendered hydrophilic by a carboxylic acid-terminated SAM. The OEG-terminated SAMs prevent the adsorption of protein on the reflective gold surface of the cantilever, whereas the acid-terminated SAMs facilitate the protein adsorption on the tip surface. The direct-write DPN process allowed the nanopatterning of two proteins (lysozyme and rabbit IgG) with no cross-contamination (Fig. 4). In this approach, protein adsorption was mainly driven by the binding of cysteine thiol residues of the proteins to the gold surface.

The properties of the gold surfaces have also allowed other thiol-containing biomolecules such as thiolated

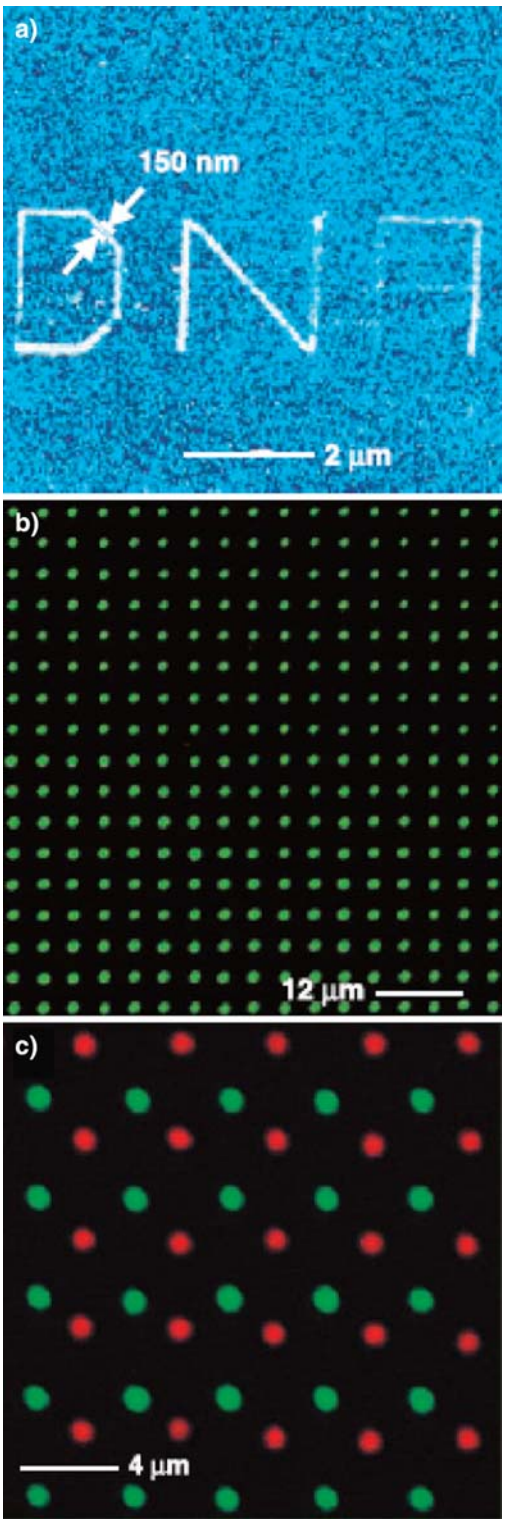

Fig. 3 **a** Atomic force microscopy tapping mode image of thiol-modified oligonucleotides DPN patterned on a gold surface [86]. **b** Epifluorescence image of fluorophore-labeled DNA hybridised to a DPN-generated pattern of complementary oligonucleotides on an oxidised silicon surface [86]. **c** Combined red–green epifluorescence image of two different fluorophore-labeled sequences simultaneously hybridised to a two-sequence array deposited on an oxidised silicon surface by DPN [86]

collagen [46] and thiol-containing peptides [46, 47, 88] to be directly immobilised on surfaces. Thiolated collagen and collagen-like peptides molecules have been patterned with line widths of 30–50 nm without the need for AFM tip modification [46]. Furthermore, the DPN deposition procedure preserved the triple-helical structure (Fig. 5) and biological activity of collagen.

Other specific binding templates have been exploited to pattern directly biomolecules on gold [84], glass [89], mica [90], oxidised silicon [85] and nickel substrates [87, 91]. For instance, gold surfaces were coated with Prolinker^{TM}, which contains crown ether moieties that can capture protonated amines in protein structures by host–guest interactions [84]. Using this strategy, nanoarrays of integrin $\alpha_v\beta_3$ and angiogenin proteins have been fabricated with feature widths of 120 and 60 nm, respectively. Glass surfaces were treated with 3-glycidoxypropyltrimethoxysilane to generate patterns of human chorionic gonadotropin antibody by direct-write DPN [89]. Protein nanoarrays with sub-100 nm features have also been fabricated onto silicon oxidised surfaces through electrostatic interactions between the positively charged parts of the protein and the pre-treated silica surface with base (rendering it negatively charged), or through covalent bonding between aldehyde-modified silicon oxidised surfaces and amine groups on the protein molecules [85].

Electrochemical DPN [91] in the tapping mode of AFM has been employed for direct immobilisation of poly-histidine-tagged peptides and proteins on nickel substrates via metal chelation. In this process, the AFM tip was first coated with the biomolecules, which were subsequently delivered to the surface by applying an electrical potential to the AFM tip. The water meniscus acted as a nanoscale electrochemical cell, causing ionisation of the nickel surface and localised binding of the poly-histidine-tagged peptides and proteins. Using a different strategy, histidine-tagged proteins (i.e. ubiquitin and thioredoxin) have also been patterned on nickel surfaces with feature sizes as small as 80 nm without the need for an applied potential during the DPN process [87]. Reliable protein transport and uniform protein patterning was achieved by coating the AFM tips with a thin layer of nickel.

DPN is a versatile tool that has been used to immobilise biomolecules such as DNA, peptides, proteins and virus on various substrates with indirect- or direct-write methods. Indirect methodologies have been effectively used to control the deposition of single biomolecules on substrates [75]. By employing direct DPN patterning, feature sizes as small as 30 nm were created [46], and it is reasonable to expect that it will rival that of conventional DPN (15 nm) [51]. Furthermore, biologically active biomolecule nanoarrays have been fabricated over macroscopic distances through parallel DPN [78]. Although two-component

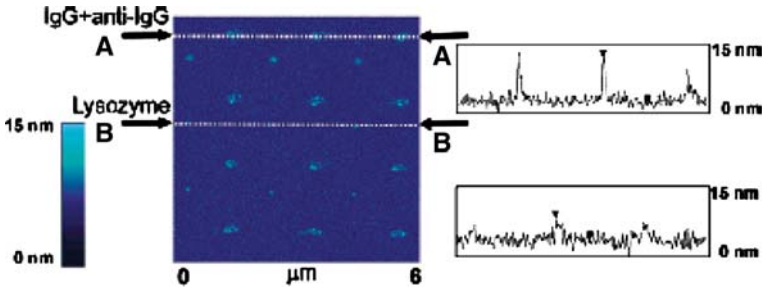

Fig. 4 Two-component protein (lysozyme and rabbit IgG) nanoarrays, in which biorecognition properties were demonstrated by selective binding of anti-rabbit IgG to rabbit IgG patterned features [52]

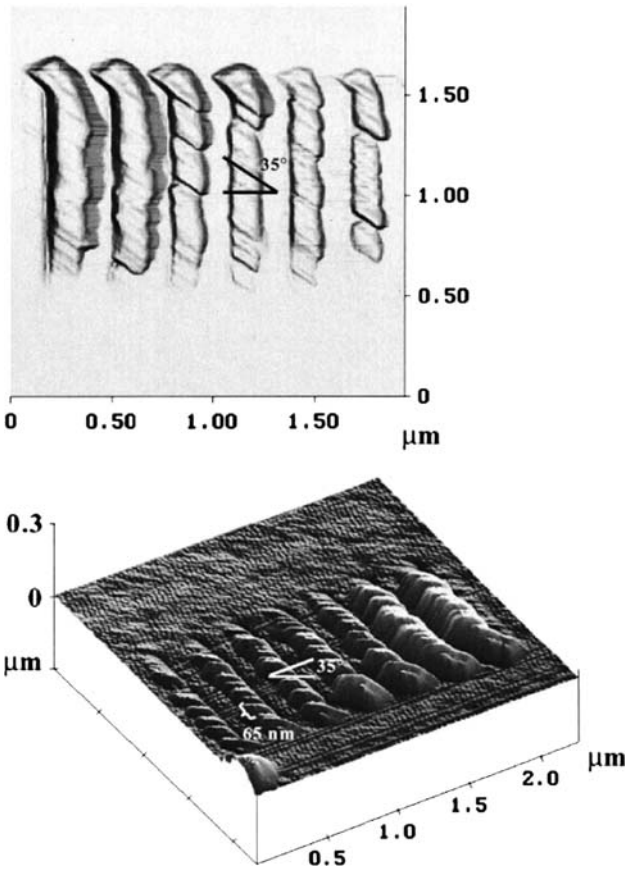

Fig. 5 Top and surface plot views of an AFM tapping mode image of modified collagen molecules deposited on Au substrates by DPN [46]

biomolecule patterns have been generated by direct-write DPN [52, 84], further equipment modification and operation will be required for fabricating extensive multicomponent arrays.

Nanoshaving

Nanoshaving is also a scanning probe microscopy-based lithographic technique, in which a resist material is mechanically removed by an AFM tip for creating nanometre scale patterns on surfaces (process C—Fig. 1). The resolution and sharpness of the patterns depends not only on local displacement, but also immediate removal of the displaced adsorbate and suppression of readsorption [92]. The possibility for nanoshaving was first explored in 1994 by Wendel et al. [93]. As well as fabricating holes, they fabricated narrow trenches in poly(methyl methacrylate) (PMMA) photoresist and gold layers. The AFM tip operating in tapping mode was used to shave away the soft gold deposited on a hard substrate leading to feature widths of approximately 50 nm. To date, these are the smallest features achieved through nanoshaving.

Nanoshaving has been combined with SAMs as nanometre thickness resists for indirect immobilisation of biomolecules on surfaces [94–98]. The nanoshaved patterned surfaces have been exploited as templates for the direct assembly of thiolated peptide nanotubes [96] and proteins on gold substrates [97, 98]. SAMs of octadecanethiol (ODT) were formed on gold surfaces, followed by nanoshaving to selectively remove ODT from specific areas on the surface [96–98]. Trenches up to 1 µm in length with widths of 150 nm were fabricated [98]. Thiol–gold interactions were then employed to immobilise the thiolated peptide nanotubes [96] and IgG proteins *via* cysteine thiol residues [97, 98] onto the patterned gold trenches. On the basis of a two-step nanoshaving and protein immobilisation process, two different antibodies (mouse IgG and human IgG) were selectively immobilised on shaved nanotrenches [98]. Anti-mouse IgG coated nanotubes and anti-human IgG coated nanotubes were shown to specifically bind to the complementary antibody-patterned surfaces.

In order to reduce the effects of non-specific protein adsorption, protein-resistant ethylene glycol SAMs have also been explored as resist materials for nanografting [99]. Protein immobilisation to the shaved regions was achieved either through the chemisorption of a disulfide coupling agent dithiobis(succinimidyl undecanoate) followed by IgG protein binding or by the direct adsorption of Fab'-SH fragment of goat anti-rabbit IgG antibody. The latter approach holds considerable promising as a means of fabricating multiple protein patterns. Even though nanoshaving does not offer extraordinary spatial resolution ($\sim$150 nm [98]) for biomolecule immobilisation on surfaces, it has the capability of being used under ambient

conditions that could prove useful for fabrication of multicomponent biomolecule nanostructures.

Nanografting

An extension to the technique of nanoshaving is that of nanografting [92, 100]. Compared to other methods of nanofabrication, nanografting allows more precise control over the size and geometry of patterned features and their location on the surface. Features as small as 2 nm × 4 nm have been reported [101]. The technique of nanografting is usually (but not exclusively) utilised on surfaces modified with SAMs and is achieved by nanoshaving in the presence of a second replacement surfactant molecule with a greater affinity for the surface than the molecule being removed by the AFM tip. Therefore, once the pre-formed SAM is removed from the desired area by the AFM tip it will be replaced with a second surfactant to form a new SAM in the patterned area. In order to successfully perform a nanografting operation, there are certain requirements that SAMs should meet. The SAMs must be readily removable with the force applied by the AFM tip, but more importantly, the second surfactant must form the new SAM rapidly. It is for these reasons that thiol SAMs on gold are usually the system of choice for nanografting experiments, due to the way in which thiols rapidly form homogenous monolayers on exposed gold surfaces. This strategy has been used for the production of nanometre-sized protein patterns on gold surfaces by exploiting the affinity of biomolecules towards different SAMs.

Indirect Nanografting

Electrostatic interactions have been exploited in conjunction with nanografting for the fabrication of protein nanopatterns [99, 102–104]. For instance, reactive carboxylic acid-terminated SAMs were nanografted into methyl-terminated SAMs on gold substrates [99, 103, 104]. Lysozyme and IgG proteins were shown to adsorb selectively on the patterned surfaces via electrostatic interactions between the negatively charged acid-terminated regions and the positively charged proteins [103, 104]. Line features as small as 10 nm × 150 nm were fabricated (Fig. 6) [103].

More stable protein patterns have also been produced by, for instance, formation of amide bonds between the nanografted acid-terminated regions and the primary amine groups in rabbit IgG using 1-ethyl-3-(3-dimethylaminopropyl)carbodiimide hydrochloride (EDC) chemistry [99]. Imine bond formation has also been exploited to covalently immobilise proteins on gold surfaces [103–105]. Nanografting was employed to incorporate aldehyde-terminated

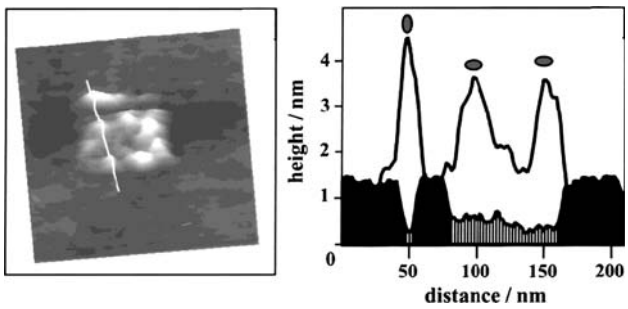

Fig. 6 Lysozyme nanopatterns with a 10 nm × 150 nm line and a 100 nm × 150 nm rectangle formed through electrostatic interactions between acid-terminated patterned surfaces generated by nanoshaving and the negatively charged lysozyme protein. The lysozyme proteins adopt different orientations when electrostatically immobilised on the surface [103]

SAMs into methyl-terminated SAMs on gold substrates [103–105]. Protein nanopatterned surfaces were subsequently produced through formation of imine bonds between the aldehyde moieties on the patterned surfaces and the primary amine groups in the IgG, lysozyme and BSA proteins [103–105]. The proteins remained bioactive on the surfaces and features as small as 40 nm × 40 nm were generated [104, 105].

Direct Nanografting

Studies have also been conducted on the direct nanografting of DNA [106] and proteins on gold surfaces via thiol–gold interaction [107, 108]. These approaches relied on a well-controlled modification of the DNA and proteins with thiol groups. Designed metal-assembled three-helix bundle metalloproteins $[Fe(\alpha pV_aL_dC26)_3]^{2+}$, in which the three-helices were specifically engineered with three cysteines groups, were not only grafted on methyl-terminated SAMs, but were also shown to adopt a vertical orientation on the gold surface [107]. Using a similar methodology, lines of DNA molecules as narrow as 10 nm were produced and molecules were also shown to adopt a standing up orientation on the gold surface [106].

Nanografting has been limited to the use of gold substrates, but it offers the possibility of immobilising biomolecules on these surfaces with resolution down to 10 nm [103]. As for DPN and nanografting, nanoshaving allows the patterning of biomolecules on surfaces under ambient conditions.

Electron-beam Lithography

Electron-beam lithography is a well developed and optimised technique for semiconductor fabrication. The

resolution of EBL is not limited by the focus of the beam (~1 nm), but by the size of the molecules in the resists and secondary electron processes, such as electron scattering and the proximity effect. EBL is capable of producing features down to 5 nm in electron-sensitive resists such as SAMs with high reliability and integral control over the location of the features [109]. Although electron-beam technology still has throughput issues, important advances have been made in the development of parallel techniques/tools such as projection e-beam lithography [110, 111] and multibeam sources [112, 113].

Electron-beam lithography has been exploited to create biological nanostructures by first patterning a pre-formed homogeneous film, and subsequently attach the biomolecules of interest. Building on well-known sensitivity of SAMs to electron irradiation [114], thiolates SAMs on gold have been selectively removed by EBL and the exposed areas used for creating bioactive templates [115, 116]. For example, PEG monolayers on gold were patterned by electron-beam to create biomolecular features with dimensions of about 40 nm [116]. Depending on the electron beam dose used, the SAM was removed from the gold surface or some carbonaceous material was deposited on the surface (i.e. contamination writing). Both patterned surfaces were shown to immobilise neutravidin-coated 40 nm FluoSpheres with high selectivity [116]. A similar electron-beam strategy was also applied to silane SAMs on Si/SiO_2 to create 250 nm patterns of DNA on these substrates [117].

Metal-oxide nanopatterns have also been formed which can subsequently direct the immobilisation of biomolecules [118, 119]. Indium-tin oxide (ITO)-glass substrates were coated with a thin layer of SiO_2, which was then electron-beam patterned to expose nanoregions of the underlying ITO. Dodecylphosphate, to which proteins can bind, was selectively adsorbed on the ITO nanostructures, whereas poly-L-lysine-*g*-poly(ethylene glycol) was used to passivate the surrounding SiO_2 regions against protein adsorption [119]. Fluorescently labelled streptavidin was shown to specifically adsorb to the hydrophobic ITO/dodecylphosphate nanopatterned surfaces (~140 nm) [119].

By combining EBL with a lift-off technique, metal nanoarrays have been created for immobilising proteins on Si/SiO_2 surfaces [120, 121]. For instance, gold arrays (1 μm to 45 nm in width) were generated for selective immobilisation of disulfide-containing 2,4-dinitrophenyl-caproate (DNP-cap) ligands [120]. The ligand patterned surfaces were shown not only to bind with high specificity to anti-DNP immunoglobulin E (IgE), but also to induce specific cellular responses when incubated with rat basophilic leukaemia mast cells [120]. PMMA, which is widely used as a lithographic positive resist, has been exploited in conjunction with EBL for immobilising IgG [122] and collagen proteins [123] on Si/SiO_2 substrates. Collagen was forced to align and assemble into continuous bundles by the anisotropic dimensions of the electron-beam nanoscale patterns (30–90 nm) [123].

Electron-beam lithography has also been carried out to activate porous silicon [124] and polycaprolactone [125] films for further biomolecule immobilisation. Exposure of the electron-beam irradiated polycaprolactone surfaces to an acrylic acid solution in the presence of Mohr's salt led to a graft polymerisation of the acrylic acid on to the polymer surface [125]. A three-step peptide immobilisation process was then used to immobilise a cysteine-terminated RGD-containing peptides onto the grafted surface. EBL has also been exploited to locally crosslink amine-terminated poly(ethylene glycol) films to create hydrogel nanoarrays with ~200 nm features on silicon substrates [126]. BSA nanoarray pads were then generated by EDC chemistry. Two different BSA hydrogel nanoarray pads with lateral dimensions of 5 μm × 5 μm on the same substrate were further employed to immobilise two different proteins, fibronectin and laminin, via a photoactivate heterobifunctional crosslinker [sulfosuccinimidyl-6-(4′-azido-2′-nitrophenylamino)hexanoate] [126].

A particularly attractive feature of using EBL for nanopatterning biomolecules is its compatibility with standard microfabrication techniques developed in the semiconductor industry, allowing the diverse functions of biomolecules to be easily integrated into, for example, bio-nanoelectromechanical systems (bioNEMS) and sensor devices. However, the principal drawbacks are that electron-beam modification occurs under ultra-high vacuum conditions, limiting the potential of this technique for multicomponent biomolecule nanopatterning.

Nanocontact Printing

Microcontact printing (μCP) [127] is widely used for generating micropatterns of nanomaterials such as organic molecules [128, 129] and biomolecules [130–134] over large surface areas (>cm^2). In the μCP process, a microstructured elastomer stamp is coated with a solution of a nanomaterial and applied to a substrate of choice. Upon contact with the substrate, the inked protrusions of the pattern of the stamp deform slightly to make intimate contact with the surface and facilitates diffusion from the stamp to the substrate [127, 135]. After a given period of time in conformal contact with the substrate, the stamp is removed leaving a replica of the stamp pattern on the substrate surface. The elastomer stamps are made typically from poly(dimethylsiloxane) (PDMS) by curing liquid prepolymers of PDMS on a lithographically prepared

master. Since μCP technique is carried out under ambient conditions, different biomolecules have been directly transferred in a controlled way onto a variety of substrates while retaining their biological activity [130–134]. By combining μCP with a microfluid network, 16 different proteins were successfully patterned into rows with micrometre dimensions [131].

More recently, μCP concept has been extended to nanoscale dimensions, a process referred to as nCP [135–137]. Features as small as 40 nm can now be fabricated by this process [136]. Nanocontact printing has been achieved by either decreasing the feature sizes in the PDMS stamp and diluting the nanomaterial inks [137], utilising special variants of PDMS stamps [135, 136] or employing new polymeric material stamps (e.g. polyolefin plastomers) [138]. Another important factor on obtaining high-resolution prints at the 100 nm level relates with the ink utilised. In this context, biomolecules are attractive nanocontact printing inks since their high molecular weight prevents diffusion during the printing step, resulting in high-resolution features.

By diluting the protein solution and decreasing the feature size of the PDMS stamp, patterns of IgG and green fluorescent proteins with 100 nm wide lines were generated on glass substrates [137]. A composite PDMS stamp, cast from V-shaped gratings used for AFM tip characterisation, was also used to print lines of titin multimer proteins on a silicon surface with widths less than 70 nm (Fig. 7) [136]. The stamp design was based on a two layer stamp that uses a thick film of standard soft PDMS (Sylgard 184 PDMS) to support a thin stiff layer of hard PDMS [135]. The hard PDMS layer improved the mechanical stability of the features on the stamp, reducing sidewall buckling and unwanted sagging from the relief features [135, 136]. New polyolefin plastomer stamps were also exploited for creating fibrinogen protein nanostructures on glass surfaces [138]. The higher stiffness of these stamps allowed that 100 nm width lines of fibrinogen could be fabricated with superior quality than those resulting from PDMS stamps [138].

A significant advantage of nCP lithography compared to serial techniques such as dip-pen lithography is that large areas can be nanopatterned rapidly. Furthermore, as opposed to the parallel conventional photolithographic process, nCP is not diffraction limited and it should be possible to pattern surfaces with molecular sized features. The technique has been able, so far, to generate protein patterns with dimensions of 70 nm [136]. Multicomponent biomolecule nanopatterning is problematic with this technology due to the practical difficulties in accurately aligning multiple flexible stamps over a large area with nanoscale resolution and thus further development is required to solve this problem.

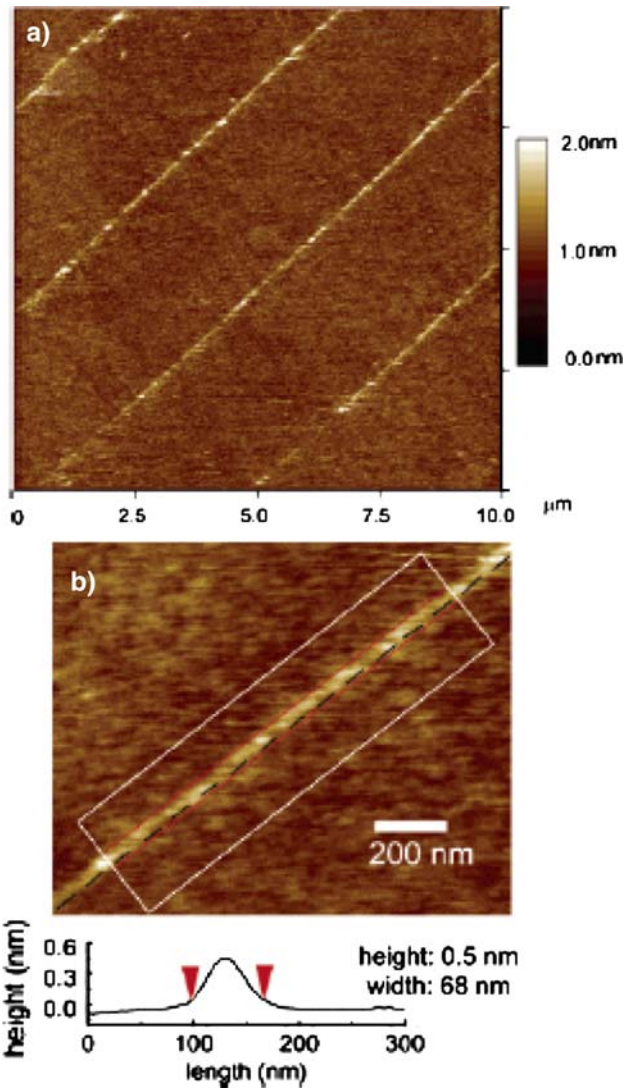

Fig. 7 AFM tapping mode images of nanocontact printed titin multimer protein lines on a silicon surface **a** at large scale and **b** at high-resolution with height profile *cross section below* [136]

Summary and Outlook

A suite of bio-nanofabrication technologies now exist for patterning a wide range of biomolecules such as DNA, peptides, proteins and viruses on many types of materials. These include DPN, nanoshaving, nanografting, EBL and nanocontact printing (Table 1). Each of these techniques has its own strengths and weaknesses with regard to resolution, patterning speed, biocompatibility, complexity, and cost. In particular, these reported strategies have the common shortcoming of not being so far suitable for nanopatterning of multiple biomolecule nanoarrays. For instance, while dip-pen lithography exhibits high reliability and precise control over the location of 30 nm biomolecule features [46] and represents the state-of-the-art presently

Table 1 Summary of the biomolecules employed and highest resolution achieved so far with the different nanolithographic techniques

	Dip-pen nanolithography		Nanoshaving	Nanografting		Electron-beam lithography	Nanocontact printing
Patterned biomolecules	Indirect	Direct		Indirect	Direct		
	DNA	DNA	Peptides	Proteins	DNA	DNA	Proteins
	Peptides	Peptides	Proteins		Proteins	Peptides	
	Proteins	Proteins				Proteins	
	Virus						
Highest resolution	~85 nm	30 nm	150 nm	10 nm	10 nm	30 nm	70 nm
	IgG protein dot features [73]	Collagen-like peptide lines [46]	IgG protein lines [98]	Lysozyme protein lines [103]	DNA lines [106]	Collagen protein lines [123]	Titin multimer protein lines [136]

for biomolecule patterning density [78], its multicomponent biomolecule patterning capabilities have been hindered by the significant complexity involving both equipment modification and operation [52, 86]. Nevertheless, nanomanufacturing processes are evolving at fast pace, with the future holding the promise of not only providing innovative solutions to existing problems, but also offering new opportunities through the development of novel bio-nanoengineered surfaces.

Further paradigm shifts will be also driven by the need for smart, bioactive and nanostructured materials, including stimuli-responsive nanostructured materials. Development of smart biological surfaces [139–141] that can modulate the spatiotemporal biological properties at the nanoscale represents a major, and exciting challenge, for the future that may lead to new breakthroughs in the biological and medical sciences and ultimately, the delivery of health care.

Acknowledgements The authors acknowledge financial support from the European Community (NANO3D.NMP-CT-2005-014006) and the Engineering and Physical Sciences Research Council (EPSRC).

References

1. C.M. Niemeyer, C.A. Mirkin (eds.), *Nanobiotechnology* (Wiley-VCH Verlag GmbH & Co. KGaA, Weinheim, 2004)
2. D. Kambhampati (ed), *Protein Microarray Technology* (Wiley-VCH Verlag GmbH & Co. KGaA, Weinheim, 2004)
3. G.F. Zheng, F. Patolsky, Y. Cui, W.U. Wang, C.M. Lieber, Nat. Biotechnol. **23**, 1294–1301 (2005)
4. G. Shekhawat, S.H. Tark, V.P. Dravid, Science **311**, 1592–1595 (2006)
5. Y. Cui, Q.Q. Wei, H.K. Park, C.M. Lieber, Science **293**, 1289–1292 (2001)
6. K.L. Christman, V.D. Enriquez-Rios, H.D. Maynard, Soft Matter **2**, 928–939 (2006)
7. V.V. Demidov, Expert Rev. Mol. Diagn. **4**, 267–268 (2004)
8. D.P. Malinowski, Expert Rev. Mol. Diagn. **7**, 117–131 (2007)
9. C.X. Lin, Y. Liu, H. Yan, Nano Lett. **7**, 507–512 (2007)
10. M.M. Ling, C. Ricks, P. Lea, Expert Rev. Mol. Diagn. **7**, 87–98 (2007)
11. M. Freemantle, Chem. Eng. News. **77**, 22–27 (1999)
12. M.M. Stevens, J.H. George, Science **310**, 1135–1138 (2005)
13. J. Sagiv, J. Am. Chem. Soc. **102**, 92–98 (1980)
14. J. Gun, R. Iscovici, J. Sagiv, J. Colloid Interface Sci. **101**, 201–213 (1984)
15. R. Maoz, J. Sagiv, J. Colloid Interface Sci. **100**, 465–496 (1984)
16. L. Netzer, J. Sagiv, J. Am. Chem. Soc. **105**, 674–676 (1983)
17. L. Netzer, R. Iscovici, J. Sagiv, J. Am. Chem. Soc. **99**, 235–241 (1983)
18. R.G. Nuzzo, D.L. Allara, J. Am. Chem. Soc. **105**, 4481–4483 (1983)
19. F. Schreiber, J. Phys. Condens. Matter **16**, R881–R900 (2004)
20. S. Onclin, B.J. Ravoo, D.N. Reinhoudt, Angew. Chem. Int. Ed. Engl. **44**, 6282–6304 (2005)
21. C.S. Fadley, R.J. Baird, W. Siekhaus, T. Novakov, S.A.L. Bergstro, J. Electron Spectrosc. Relat. Phenom. **4**, 93–137 (1974)
22. Surface Analysis by Auger and X-Ray Photoelectron Spectroscopy (SurfaceSpectra Ltd and IM Publications, Manchester, 2003)
23. J. Alsnielsen, D. Jacquemain, K. Kjaer, F. Leveiller, M. Lahav, L. Leiserowitz, Phys. Rep. Rev. Sec. Phys. Lett. **246**, 252–313 (1994)
24. R.J. Good, J. Adhes. Sci. Technol. **6**, 1269–1302 (1992)
25. F.L. McCrackin, E. Passaglia, R.R. Stromberg, H.L. Steinber, (1963) J. Res. Nat. Bur. Stand. A **67**, 363
26. G. Binning, H. Rohrer, Ch. Gerber, E. Weibel, Phys. Rev. Lett. **49**, 57–61 (1982)
27. G. Binning, C.F. Quate, Ch. Gerber, Phys. Rev. Lett. **56**, 930–933 (1986)
28. T. Uchihashi, T. Ishida, M. Koomiyama, M. Ashino, Y. Sugawara, W. Mizutani, K. Yokoyama, S. Morita, H. Tokumoto, M. Ishikawa, Appl. Surf. Sci. **157**, 244–250 (2000)
29. P.M. Mendes, S. Jacke, K. Critchley, J. Plaza, Y. Chen, K. Nikitin, R.E. Palmer, J.A. Preece, S.D. Evans, D. Fitzmaurice, Langmuir **20**, 3766–3768 (2004)
30. P. Mendes, M. Belloni, M. Ashworth, C. Hardy, K. Nikitin, D. Fitzmaurice, K. Critchley, S. Evans, J. Preece, Chemphyschem **4**, 884–889 (2003)
31. P.M. Mendes, J.A. Preece, Curr. Opin. Colloid Interface Sci. **9**, 236–248 (2004)
32. J. Groll, K. Albrecht, P. Gasteier, S. Riethmueller, U. Ziener, M. Moeller, Chembiochem **6**, 1782–1787 (2005)
33. A. Valsesia, P. Colpo, T. Meziani, P. Lisboa, M. Lejeune, F. Rossi, Langmuir **22**, 1763–1767 (2006)

34. F.A. Denis, P. Hanarp, D.S. Sutherland, Y.F. Dufrene, Langmuir **20**, 9335–9339 (2004)
35. R. Michel, I. Reviakine, D. Sutherland, C. Fokas, G. Csucs, G. Danuser, N.D. Spencer, M. Textor, Langmuir **18**, 8580–8586 (2002)
36. Y.G. Cai, B.M. Ocko, Langmuir **21**, 9274–9279 (2005)
37. H. Agheli, J. Malmstrom, E.M. Larsson, M. Textor, D.S. Sutherland, Nano Lett. **6**, 1165–1171 (2006)
38. H. Yan, S.H. Park, G. Finkelstein, J.H. Reif, T.H. LaBean, Science **301**, 1882–1884 (2003)
39. C.S. Lee, S.E. Baker, M.S. Marcus, W.S. Yang, M.A. Eriksson, R.J. Hamers, Nano Lett. **4**, 1713–1716 (2004)
40. J.H. Gu, C.M. Yam, S. Li, C.Z. Cai, J. Am. Chem. Soc. **126**, 8098–8099 (2004)
41. S.Q. Sun, M. Montague, K. Critchley, M.S. Chen, W.J. Dressick, S.D. Evans, G.J. Leggett, Nano Lett. **6**, 29–33 (2006)
42. D. Falconnet, D. Pasqui, S. Park, R. Eckert, H. Schift, J. Gobrecht, R. Barbucci, M. Textor, Nano Lett. **4**, 1909–1914 (2004)
43. J.D. Hoff, L.J. Cheng, E. Meyhofer, L.J. Guo, A.J. Hunt, Nano Lett. **4**, 853–857 (2004)
44. V.N. Truskett, M.P.C. Watts, Trends Biotechnol. **24**, 312–317 (2006)
45. R.D. Piner, J. Zhu, F. Xu, S. Hong, C.A. Mirkin, Science **283**, 661–663 (1999)
46. D.L. Wilson, R. Martin, S. Hong, M. Cronin-Golomb, C.A. Mirkin, D.L. Kaplan, Proc. Natl. Acad. Sci. U.S.A. **98**, 13660–13664 (2001)
47. G. Agarwal, L.A. Sowards, R.R. Naik, M.O. Stone, J. Am. Chem. Soc. **125**, 580–583 (2002)
48. R.D. Piner, C.A. Mirkin, Langmuir **13**, 6864–6868 (1997)
49. B.L. Weeks, M.W. Vaughn, J.J. DeYoreo, Langmuir **21**, 8096–8098 (2005)
50. D.S. Ginger, H. Zhang, C.A. Mirkin, Angew. Chem. Int. Ed. Engl. **43**, 30–45 (2004)
51. S.H. Hong, J. Zhu, C.A. Mirkin, Science **286**, 523–525 (1999)
52. K.B. Lee, J.H. Lim, C.A. Mirkin, J. Am. Chem. Soc. **125**, 5588–5589 (2003)
53. P.E. Sheehan, L.J. Whitman, Phys. Rev. Lett. **88**, 156104 (2002)
54. P. Manandhar, J. Jang, G.C. Schatz, M.A. Ratner, S. Hong, Phys. Rev. Lett. **90**, 115505 (2003)
55. B.L. Weeks, A.E. Miller, J.J. De Yoreo, Phys. Rev. Lett. **88**, 255505 (2002)
56. J.R. Hampton, A.A. Dameron, P.S. Weiss, J. Phys. Chem. B **109**, 23118–23120 (2005)
57. J.R. Hampton, A.A. Dameron, P.S. Weiss, J. Am. Chem. Soc. **128**, 1648–1653 (2006)
58. P. Vettiger, M. Despont, U. Drechsler, U. Dürig, W. Häberle, M.I. Lutwyche, H.E. Rothuizen, R. Stutz, R. Widmer, G.K. Binnig, IBM J. Res. Dev. **44**, 323–340 (2000)
59. K. Salaita, S.W. Lee, X. Wang, L. Huang, T.M. Dellinger, C. Liu, C.A. Mirkin, Small **1**, 940–945 (2005)
60. M. Zhang, D. Bullen, S.-W. Chung, S. Hong, K.S. Ryu, Z. Fan, C.A. Mirkin, C. Liu, Nanotechnology **13**, 212–217 (2002)
61. S.H. Hong, C.A. Mirkin, Science **288**, 1808–1811 (2000)
62. C.A. Mirkin, S. Hong, L. Demers, Chemphyschem **2**, 37–39 (2001)
63. F. Stellacci, Adv. Funct. Mater. **16**, 15–16 (2006)
64. D. Bullen, C. Liu, Sens. Actuators A Phys. **125**, 504–511 (2006)
65. K.-H. Kim, C. Ke, N. Molodovan, H.D. Espinosa, *Massively Parallel Multi-Tip Nanoscale Writer with Fluidic Capabilities—Fountain Pen Nanolithography (FPN)*. 4th International Symposium on MEMS and Nanotechnology, Charlotte, 2003, pp. 235–238
66. Y. Zhang, K. Salaita, J.H. Lim, K.B. Lee, C.A. Mirkin, Langmuir **20**, 962–968 (2004)
67. K. Salaita, Y. Wang, J. Fragala, R.A. Vega, C. Liu, C.A. Mirkin, Angew. Chem. Int. Ed. Engl. **118**, 7378–7381 (2007)
68. D. Nyamjav, A. Ivanisevic, Adv. Mater. **15**, 1805–1809 (2003)
69. D. Nyamjav, A. Ivanisevic, Biomaterials **26**, 2749–2757 (2005)
70. R. Valiokas, S. Vaitekonis, G. Klenkar, G. Trinkũnas, B. Lindberg, Langmuir **22**, 3456–3460 (2006)
71. K.B. Lee, S.J. Park, C.A. Mirkin, J.C. Smith, M. Mrksich, Science **295**, 1702–1705 (2002)
72. H. Zhang, K.-B. Lee, Z. Li, C.A. Mirkin, Nanotechnology **14**, 1113–1117 (2003)
73. K.B. Lee, E.Y. Kim, C.A. Mirkin, S.M. Wolinsky, Nano Lett. **4**, 1869–1872 (2004)
74. J.C. Smith, K.-B. Lee, Q. Wang, M.G. Finn, J.E. Johnson, M. Mrksich, C.A. Mirkin, Nano Lett. **3**, 883–886 (2003)
75. R.A. Vega, D. Maspoch, K. Salaita, C.A. Mirkin, Angew. Chem. Int. Ed. Engl. **44**, 6013–6015 (2005)
76. L.M. Demers, S.J. Park, T.A. Taton, Z. Li, C.A. Mirkin, Angew. Chem. Int. Ed. Engl. **40**, 3071–3073 (2001)
77. J. Hyun, W.-K. Lee, N. Nath, A. Chilkoti, S. Zauscher, J. Am. Chem. Soc. **126**, 7330–7335 (2004)
78. S.W. Lee, B.K. Oh, R.G. Sanedrin, K. Salaita, T. Fujigaya, C.A. Mirkin, Adv. Mater. **18**, 1133–1136 (2006)
79. J. Hyun, S.J. Ahn, W.K. Lee, A. Chilkoti, S. Zauscher, Nano Lett. **2**, 1203–1207 (2002)
80. N.M. Green, Adv. Protein Chem. **29**, 85–133 (1975)
81. D.J. Pena, M.P. Raphael, J.M. Byers, Langmuir **19**, 9028–9032 (2003)
82. H. Jung, R. Kulkarni, C.P. Collier, J. Am. Chem. Soc. **125**, 12096–12097 (2003)
83. C.L. Cheung, J.A. Camero, B.W. Woods, T. Li, J.E. Johnson, J.J. De Yoreo, J. Am. Chem. Soc. **125**, 6848–6849 (2003)
84. M. Lee, D.K. Kang, H.K. Yang, K.H. Park, S.Y. Choe, C.S. Kang, S.I. Chang, M.H. Han, I.C. Kang, Proteomics **6**, 1094–1103 (2006)
85. J.-H. Lim, D.S. Ginger, K.-B. Lee, J. Heo, J.-M. Nam, C.A. Mirkin, Angew. Chem. Int. Ed. Engl. **42**, 2309–2312 (2003)
86. L.M. Demers, D.S. Ginger, S.J. Park, Z. Li, S.W. Chung, C.A. Mirkin, Science **296**, 1836–1838 (2002)
87. J.M. Nam, S.W. Han, K.-B. Lee, X. Liu, M.A. Ratner, C.A. Mirkin, Angew. Chem. Int. Ed. Engl. **43**, 1246–1249 (2004)
88. Y. Cho, A. Ivanisevic, J. Phys. Chem. B **109**, 6225–6232 (2005)
89. A. Noy, A.E. Miller, J.E. Klare, B.L. Weeks, B.W. Woods, J.J. DeYoreo, Nano Lett. **2**, 109–112 (2002)
90. B. Li, Y. Zhang, J. Hu, M. Li, Ultramicroscopy **105**, 312–315 (2005)
91. G. Agarwal, R.R. Naik, M.O. Stone, J. Am. Chem. Soc. **125**, 7408–7412 (2003)
92. G.-Y. Liu, S. Xu, Y. Qian, Acc. Chem. Res. **33**, 457–466 (2000)
93. M. Wendel, S. Kuhn, H. Lorenz, J.P. Kotthaus, M. Holland, Appl. Phys. Lett. **65**, 1775–1777 (1994)
94. M. Kaholek, W.K. Lee, B. LaMattina, K.C. Caster, S. Zauscher, Nano Lett. **4**, 373–376 (2004)
95. J.E. Headrick, M. Armstrong, J. Cratty, S. Hammond, B.A. Sheriff, C.L. Berrie, Langmuir **21**, 4117–4122 (2005)
96. I.A. Banerjee, L. Yu, R.I. MacCuspie, H. Matsui, Nano Lett. **4**, 2437–2440 (2004)
97. N. Nuraje, I.A. Banerjee, R.I. MacCuspie, L. Yu, H. Matsui, J. Am. Chem. Soc. **126**, 8088–8089 (2004)
98. Z. Zhao, I.A. Banerjee, H. Matsui, J. Am. Chem. Soc. **127**, 8930–8931 (2005)
99. J.R. Kenseth, J.A. Harnisch, V.W. Jones, M.D. Porter, Langmuir **17**, 4105–4112 (2001)
100. S. Xu, G.Y. Liu, Langmuir **13**, 127–129 (1997)
101. S. Xu, S. Miller, P.E. Laibinis, G.Y. Liu, Langmuir **15**, 7244–7251 (1999)

102. D.J. Zhou, X. Wang, L. Birch, T. Rayment, C. Abell, Langmuir **19**, 10557–10562 (2003)
103. K. Wadu-Mesthrige, S. Xu, N.A. Amro, G.-Y. Liu, Langmuir **15**, 8580–8583 (1999)
104. K. Wadu-Mesthrige, N.A. Amro, J.C. Garno, S. Xu, G.-Y. Liu, Biophys. J. **80**, 1891–1899 (2001)
105. G.-Y. Liu, N.A. Amro, Proc. Natl. Acad. Sci. U.S.A. **99**, 5165–5170 (2002)
106. M.Z. Liu, N.A. Amro, C.S. Chow, G.Y. Liu, Nano Lett. **2**, 863–867 (2002)
107. Y. Hu, A. Das, M.H. Hecht, G. Scoles, Langmuir **21**, 9103–9109 (2005)
108. M.A. Case, G.L. McLendon, Y. Hu, T.K. Vanderlick, G. Scoles, Nano Lett. **3**, 425–429 (2003)
109. M.J. Lercel, C.S. Whelan, H.G. Craighead, K. Seshadri, D.L. Allara, J. Vac. Sci. Technol. B **14**, 4085–4090 (1996)
110. L.R. Harriott, J. Vac. Sci. Technol. B **15**, 2130–2135 (1997)
111. N. Samoto, A. Yoshida, H. Takano, A. Endo, T. Fukui, J. Microlithogr. Microfabr. Microsyst. **4** (2005)
112. J.P. Spallas, C.S. Silver, L.P. Muray, J. Vac. Sci. Technol. B **24**, 2892–2896 (2006)
113. T. Haraguchi, T. Sakazaki, S. Hamaguchi, H. Yasuda, J. Vac. Sci. Technol. B **20**, 2726–2729 (2002)
114. P.M. Mendes, J.A. Preece, Curr. Opin. Colloid Interface Sci. **9**, 236–248 (2004)
115. C.K. Harnett, K.M. Satyalakshmi, H.G. Craighead, Langmuir **17**, 178–182 (2001)
116. J. Rundqvist, J.H. Hoh, D.B. Haviland, Langmuir **22**, 5100–5107 (2006)
117. G.J. Zhang, T. Tanii, T. Funatsu, I. Ohdomari, Chem. Commun. 786–787 (2004)
118. J.W. Lussi, C. Tang, P.-A. Kuenzi, U. Staufer, G. Csucs, J. Voros, G. Danuser, J. Hubbell, M. Textor, Nanotechnology **16**, 1781–1786 (2005)
119. P.A. Kunzi, J. Lussi, L. Aeschimann, G. Danuser, M. Textor, N.F. de Rooij, U. Staufer, Microelectron. Eng. **78–79**, 582–586 (2005)
120. W. Senaratne, P. Sengupta, V. Jakubek, D. Holowka, C.K. Ober, B. Baird, J. Am. Chem. Soc. **128**, 5594–5595 (2006)
121. O. Cherniavskaya, C.J. Chen, E. Heller, E. Sun, J. Provezano, L. Kam, J. Hone, M.P. Sheetz, S.J. Wind, J. Vac. Sci. Technol. B **23**, 2972–2978 (2005)
122. T. Powell, J.Y. Yoon, Biotechnol. Prog. **22**, 106–110 (2006)
123. F.A. Denis, A. Pallandre, B. Nysten, A.M. Jonas, C.C. Dupont-Gillain, Small **1**, 984–991 (2005)
124. S. Borini, S. D'Auria, M. Rossi, A.M. Rossi, Lab Chip **10**, 1048–1052 (2005)
125. S. Hui, A. Wirsen, A.C. Albertsson, Biomacromolecules **5**, 2275–2280 (2004)
126. Y. Hong, P. Krsko, M. Libera, Langmuir **20**, 11123–11126 (2004)
127. A. Kumar, G.M. Whitesides, Appl. Phys. Lett. **63**, 2002–2004 (1993)
128. B.D. Gates, Q.B. Xu, M. Stewart, D. Ryan, C.G. Willson, G.M. Whitesides, Chem. Rev. **105**, 1171–1196 (2005)
129. B.D. Gates, Q.B. Xu, J.C. Love, D.B. Wolfe, G.M. Whitesides, Annu. Rev. Mater. Res. **34**, 339–372 (2004)
130. A. Bernard, E. Delamarche, H. Schmid, B. Michel, H.R. Bosshard, H. Biebuyck, Langmuir **14**, 2225–2229 (1998)
131. A. Bernard, J.P. Renault, B. Michel, H.R. Bosshard, E. Delamarche, Adv. Mater. **12**, 1067–1070 (2000)
132. D.I. Rozkiewicz, Y. Kraan, M.W.T. Werten, F.A. Wolf, V. Subramaniam, B.J. Ravoo, D.N. Reinhoudt, Chem. Eur. J. **12**, 6290–6297 (2006)
133. J.D. Gerding, D.M. Willard, A. VanOrden, J. Am. Chem. Soc. **127**, 1106–1107 (2005)
134. H.D. Inerowicz, S. Howell, F.E. Regnier, R. Reifenberger, Langmuir **18**, 5263–5268 (2002)
135. T.W. Odom, J.C. Love, D.B. Wolfe, K.E. Paul, G.M. Whitesides, Langmuir **18**, 5314–5320 (2002)
136. H.W. Li, B.V.O. Muir, G. Fichet, W.T.S. Huck, Langmuir **19**, 1963–1965 (2003)
137. J.P. Renault, A. Bernard, A. Bietsch, B. Michel, H.R. Bosshard, E. Delamarche, M. Kreiter, B. Hecht, U.P. Wild, J. Phys. Chem. B **107**, 703–711 (2003)
138. G. Csucs, T. Kunzler, K. Feldman, F. Robin, N.D. Spencer, Langmuir **19**, 6104–6109 (2003)
139. M. Mrksich, MRS Bull. **30**, 180–184 (2005)
140. S.J. Toddab, D. Farrarc, J.E. Goughb, R.V. Ulijn, Soft Matter **5**, 547–550 (2007)
141. W.-S. Yeo, M. Mrksich, Langmuir **22**, 10816–10820 (2006)